Structure and Elasticity of Polyurethane Networks. 5. Effect of Diluent in the Formation of Model Networks of Poly(oxypropylene)triol and 4,4′-Methylenebis(phenyl isocyanate)†

Michal Ilavský and Karel Dušek*

Institute of Macromolecular Chemistry, Czechoslovak Academy of Sciences, Prague 6, Czechoslovakia. *Received November 15, 1985*

ABSTRACT: The sol fraction mechanical and optical behavior of polyurethane networks prepared from a poly(oxypropylene)triol (PPT) (1,2,3-tris{ω-hydroxypoly[oxy(methyl-1,2-ethanediyl)]}propane) and 4,4′-methylenebis(phenyl isocyanate) (MDI) were investigated at various initial molar ratios of reactive groups, r_H = [OH]/[NCO] ($1 \le r_H \le 1.6$) and at various dilutions in xylene (the volume fraction of the diluent (xylene) v_d^0 was 0–0.6). The reaction proceeded in the presence of an organotin catalyst to the highest conversion of NCO groups. Mechanical measurements carried out on these networks after preparation (containing xylene) and drying proved the effect of diluent at network formation on the reduction of the equilibrium dry modulus G. A comparison between experimental results and the theory of branching processes (TBP) led to the following results: (1) With increasing dilution the fraction of bonds lost in elastically inactive cycles (EIC), s_g, increases from 0.02 to 0.06. The agreement between theoretical and experimental values of the sol fraction, w_s, is comparatively good; at higher dilutions, positive deviations of the theoretical w_s values from the experimental ones can be noticed. (2) The experimental values of the modulus G lie in the range between those theoretically predicted for the front factor $A = 1$ and $A = {}^1/_3$. Positive deviations from the value of G calculated for $A = {}^1/_3$ can be described in terms of the trapped entanglements theory over a wide range of r_H and v_d^0. (3) The generalized dependence of the reduced modulus on the weight fraction of the gel also agrees with the interpretation by the contribution of trapped entanglements to the modulus.

Introduction

It is known that the addition of diluent in the formation of polymer networks enhances cyclization and weakens interchain interactions. This is reflected in a decrease in the molecular weight of the reaction products (at the same conversion of functional groups) before the gel point, in the displacement of the latter toward higher conversions, in an increased sol content, and in a decreased equilibrium dry modulus in the rubbery region. In some cases, the addition of diluent may bring about the formation of inhomogeneities, or even phase separation. While the effect of diluent on molecular weights, gel point and sol fraction is given by an increased extent of cyclization, the decrease in the equilibrium modulus can reflect both the loss of the number of effective cross-links in the cycles and the weakening of interchain constraints. The extent of cyclization depends, in addition to the distance between functional groups and the flexibility of bond sequences that connect them, predominantly on the reaction mechanism. While in networks formed by the cross-linking chain copolymerization the cyclization may be very strong,[1] its extent in networks formed by alternating reactions from oligomers (endlinking) in the absence of diluent is comparatively weak.[2] However, dilution may considerably increase the cyclization in such systems, too.

There are several theoretical approaches to the treatment of cyclization in nonlinear polymerizations. Stepto[3] has improved Kilb's theory of the effect of cyclization on gel conversion. In this approach it is assumed that the probability of bond formation is weighted by the probability of structure propagation. The other reaction alternative consists in ring closure between unreacted functional groups connected by a sequence of units. This approach is in no way related to the history (kinetics) of the cluster formation; it is assumed that the probability of cyclization is the same for all bonds, irrespective of the state (degree of reaction) of the units from which the bond issues. Differences in the cluster symmetry are not considered either.

An exact numerical solution to the kinetic equations for nonlinear polyaddition involving cyclization is feasible to very low conversions only, due to the complexity of the molecules formed.[4] The process of formation and the complexity of structures is accounted for in the statistical theory based on cascade substitution[5] (spanning-tree approximation). The branched structures are generated from units, the states of which differ in the number of functional groups still unreacted and in the number of groups that participate either in branching or in forming a ring with one of the reacted functional groups on the same unit. The distribution of units with respect to their states is obtained by solving a limited number of kinetic differential equations (cf. ref 5 and the references therein). A disadvantage of the spanning-tree approximation is the fact that in the cascade substitution any information on the ring size (i.e., on long-range correlations), which is approximately considered in kinetic equations for the distribution of structural units, is lost.

So far, the formation of cyclic structures is probably best expressed by off-lattice computer simulation in a tridimensional space[6] used for endlinking of prepolymers. In the pregel state, it allows us to obtain a comparatively detailed information on the content of the individual cyclic structures.

However, none of the theories mentioned above considers the influence of the already existing cycles on the cyclization probability. The effects on the resulting network structure may be important in the case of a major extent of cyclization.

While the definition of cyclization is unambiguous before the gel point, the situation in the postgel state is different. The pregel definition is still valid for the sol and for dangling ends of the gel, but the gel contains many circuits with elastically active chains that determine the cycle rank and thus also the equilibrium elasticity. Some of the cycles thus formed are only singly connected with elastically active chains and act as elastically inactive cycles. (The condition for a cycle to be elastically inactive is that it must

† Dedicated to Dr. B. Sedláček on the occasion of his 60th birthday.

0024-9297/86/2219-2139$01.50/0

not contain any unit issuing more than two independent paths to infinity.) In more complicated cyclic structures the chains need not exhibit the same retractive force on deformation. In addition, elastically inactive cycles may become activated during the reaction if one of their segments is attached to the gel.[5,7] These factors were approximately considered in the cascade treatment of the spanning-tree approximation.[5] Within this approximation, the suggested procedure may be used independently of the extent of cyclization in the calculation of the extent of cyclization, sol content, and concentration of elastically active network chains (EANC) which determines the equilibrium modulus of elasticity. On the contrary, when expressing the effect of cyclization on the equilibrium modulus, Stepto[8] considered only the smallest possible rings, and their concentration was assumed to be the same as at the gel point; Leung and Eichinger[6] also considered only the smallest rings. This is a reasonable approximation only if the smallest rings prevail in the population of the elastically inactive rings, which may not be satisfied in the case of a more pronounced cyclization, e.g., at a higher dilution of the reacting system.

It is obvious that with increasing dilution during network formation, in addition to a decrease in the concentration of elastically active chains (EANCs), the dilation factor (operative in extracted and dried networks) is also affected and, in particular, the contribution to the modulus due to interchain constraints is reduced. In Flory's theory[9] the parameter κ, which determines the magnitude of these constraints, is implicitly affected by dilution. As will be shown below, the reduction of interchain constraints can be expressed with comparative ease by using the Langley–Graessley theory of trapped entanglements.[10,11] In this approximation, the contribution of interchain constraints is proportional to the probability of contacts between pairs of segments in EANCs related to the state of a perfect network without diluent. This probability increases with the square of the volume fraction of the polymer during network formation.[12]

Polyurethane networks prepared from poly(oxypropylene)triols and 4,4′-methylenebis(phenyl isocyanate) (MDI) in the absence of diluent have already been used by the present authors in studies of network formation and elasticity.[12-17] The critical conversion at gelation, sol fraction, and equilibrium elastic behavior could be well correlated with the results of the branching theory for stoichiometric systems or excess of hydroxyl groups where additional cross-linking due to side reactions did not interfere. The formation of elastically inactive cycles (EIC) and its effect on the sol fraction and equilibrium elasticity were taken into account by using the statistical theory mentioned above.[5] For interpreting the elasticity behavior, several competing rubber elasticity theories exist, and for the purpose of analyzing the experimental data a generalized plot of reduced equilibrium modulus against the gel fraction has proved to be useful.[12] In this plot, the uncertainties in the final conversion of minority groups, initial composition, and reduction of the concentration of elastically active chains by cyclization can be minimized. The analysis revealed that the modulus of a part of polyurethane networks was considerably higher than that which would correspond to the upper limit of the Flory theory,[9] i.e., to the front factor $A = 1$ (affine deformation). Therefore, this theory considering interchain constraints as affecting only junction fluctuations was found to be inapplicable to these systems. However, the experimental results could be reasonably well described by the Langley–Graessley[10,11] trapped-entanglement approach. A good correlation was obtained if the trapped-entanglement contribution was considered additive to the phantom network modulus, a procedure used by several authors (cf., e.g., ref 18–21).

In this study, we examine the sol fraction and equilibrium photoelasticity of polyurethane networks from a poly(oxypropylene)triol and 4,4′-methylenebis(phenyl isocyanate) prepared with various molar ratios of OH to NCO groups and concentrations of the diluent (xylene) present during network formation. The results are compared with predictions of the statistical branching theory, which takes into account formation of elastically inactive cycles.[5] The possibility of distinguishing between the effects of the diluent on the decrease in the concentration of elastically active network chains (EANC) and weakening of the interchain interactions is one of the aims of this study.

Experimental Section

Sample Preparation. The samples were prepared from poly(oxypropylene)triol (PPT) Niax LHT-240 (Union Carbide) from which water had been removed by azeotropic distillation with benzene; the content of residual water was 0.005 wt %. The number-average molecular weight was $M_n = 708$, the content of OH groups was 6.94 wt %, and the number-average functionality was $f_n = 2.89 \pm 0.02$; the procedure used for characterization of the PPT has been described earlier.[12] 4,4′-Methylenebis(phenyl isocyanate) (MDI) was purified by distillation under reduced pressure and twofold crystallization from hexane; the purity of MDI was 99.5%. Xylene, analytical purity grade, was dried.

Six series of networks were prepared having varying ratios r_H = [OH]/[NCO] = 1, 1.15, 1.30, 1.40, 1.50, 1.60 and varying volume fractions of the diluent during network formation, $v_d^0 = 0$, 0.2, 0.4, 0.5, and 0.6. In the process of preparation of diluted samples with $v_d^0 \geq 0.4$, MDI was dissolved in xylene at room temperature under dry nitrogen, PPT was added, and the mixture was stirred for 10 min; 0.08 wt % of dibutyltin dilaurate was then added. The polymerization proceeded in glass molds, 10 × 10 × 0.2 cm in size, first for 5 h at room temperature and then for 24 h at 70 °C. For samples with $v_d^0 = 0$ and 0.2, PPT and MDI were dosed, and the mixture was stirred for 15 min under dry nitrogen at 50 °C. After that, xylene with the catalyst was added, the mixture was homogenized, and the polymerization then proceeded in Teflon molds at 70 °C for 30 h. The compositions of the samples are given in Table I.

Extraction and Photoelastic Measurement. After the polymerization, the samples were weighed and dried under reduced pressure to constant weight, first at room temperature and then at 70 °C. The dry samples were extracted in benzene at room temperature and then additionally dried under reduced pressure at 60 °C; on drying, the weight fraction of the sol, w_s, was determined (Table I). The refractive indices were measured with an Abbé refractometer.

Photoelastic measurements were carried out by using an apparatus described earlier[21,22] in which the force, f, and the birefringence, Δn, can be determined simultaneously. The dependence of stress, $\sigma = f/A$ (A being the deformed cross-section of the sample), and of birefringence Δn on elongation, λ (= l/l_0, l and l_0 respectively being the deformed and initial sample length), was measured in the range $1 < \lambda < 1.1$ (using at least 10 λ values). The dependences of force and birefringence were read off each time after 120 s of relaxation at the given λ values; such a time of relaxation was sufficient to reach equilibrium with all the networks. The initial equilibrium shear modulus G, the deformation–optical function B, and the stress–optical coefficient $C = B/G$ were determined from

$$\sigma = G(\lambda^2 - \lambda^{-1}) \quad (1)$$

$$\Delta n = B(\lambda^2 - \lambda^{-1}) \quad (2)$$

The measurements were carried out by using both diluted samples after completed polymerization (containing xylene) (Table I, values G_p, C_p) at temperature $T_1 = 25$ °C and unextracted networks still containing sol after xylene was removed by drying (Table I, values G_d, C_d) at $T_2 = 60$ °C.

Table I
Mechanical and Optical Characteristics of Networks

sample	r_H[a]	v^0[b]	w_s[c]	G_p[d] × 10, MPa	C_p × 10^4, MPa^{-1}	G_d[d] × 10, MPa	C_d × 10^4, MPa^{-1}	ξ_I[e]	X_I[f]	s[g]	ν_{eg}[h] × 10^{-4}, mol cm^{-3}	$T_{eg}^{(2)}$[i] × 10
1	1.0	1.0	0.0008			22.6	34.9	0.997	0.981	0.024	11.96	9.22
2		0.8	0.0015	17.8	36.7	21.1	34.9	0.997	0.981	0.028	11.05	5.67
3		0.6	0.0031	11.3	38.7	15.1	35.0	0.991	0.975	0.035	9.92	3.03
4		0.5	0.0041	9.09	38.3	11.8	35.6	0.991	0.975	0.041	9.47	2.07
5		0.4	0.0064	6.74	38.7	9.39	34.5	0.988	0.972	0.049	8.73	1.27
6	1.15	1.0	0.0190			16.6	33.2	0.995	0.978	0.019	6.27	6.73
7		0.8	0.0205	11.0	36.5	13.1	35.7	0.996	0.979	0.024	6.08	4.25
8		0.6	0.0212	6.72	35.9	9.15	36.7	1.000	0.983	0.031	5.77	2.39
9		0.5	0.0231	4.79	35.2	7.01	36.6	1.002	0.985	0.037	5.52	1.56
10		0.4	0.0310	3.67	38.0	5.37	36.6	1.005	0.988	0.045	5.16	1.02
11	1.30	1.0	0.0770			8.13	33.1	0.986	0.967	0.018	3.20	4.03
12		0.8	0.0842	5.41	35.6	6.58	33.4	0.986	0.967	0.022	3.00	2.46
13		0.6	0.0952	3.27	35.9	4.24	33.8	0.988	0.969	0.029	2.77	1.32
14		0.5	0.1040	2.11	36.1	3.14	34.4	0.999	0.970	0.035	2.58	0.96
15		0.4	0.1220	1.47	37.1	2.20	35.2	1.000	0.981	0.043	2.28	0.59
16	1.40	1.0	0.1274			4.32	33.7	0.997	0.978	0.018	2.21	3.02
17		0.8	0.1394	2.58	35.1	3.41	33.8	0.997	0.978	0.022	2.04	1.82
18		0.6	0.1450	1.65	36.0	2.21	34.4	1.002	0.983	0.029	1.95	1.02
19		0.5	0.1590	1.00	37.6	1.58	33.5	1.003	0.984	0.035	1.79	0.66
20		0.4	0.1755	0.607	37.3	0.911	34.4	1.006	0.987	0.043	1.62	0.40
21	1.50	1.0	0.2400			1.59	33.0	0.994	0.975	0.017	1.08	1.54
22		0.8	0.2490	0.952	37.0	1.20	33.3	0.997	0.978	0.022	1.07	0.98
23		0.6	0.2605	0.653	36.2	0.810	33.0	0.999	0.982	0.029	0.99	0.53
24		0.5	0.2675	0.418	36.0	0.563	32.2	1.005	0.986	0.034	0.96	0.36
25		0.4	0.3020	0.179	35.9	0.279	32.5	1.006	0.987	0.042	0.77	0.20
26	1.60	1.0	0.4078			0.399	35.0	0.992	0.972	0.017	0.45	0.56
27		0.8	0.4253	0.186	38.0	0.248	31.7	0.994	0.994	0.021	0.43	0.34
28		0.6	0.4403	0.121	37.2	0.178	33.0	0.999	0.979	0.028	0.38	0.18
29		0.5	0.4633	0.072	38.3	0.120	32.3	1.001	0.981	0.033	0.33	0.11
30		0.4	0.4804	0.045	38.2	0.071	33.9	1.007	0.987	0.041	0.30	0.07

[a] r_H = [OH]/[NCO]. [b] $v^0 = 1 - v_d^0$, v_d^0 is the volume fraction of the diluent during network formation. [c] w_s is the weight fraction of the sol. [d] G_p and G_d are the equilibrium shear moduli measured after the preparation and after the drying of the sample respectively. [e] ξ_I is the conversion of NCO groups calculated from w_s by using eq 5. [f] X_I is the effective conversion of NCO groups calculated from w_s by using eq 20, ref 5. [g] s is the calculated fraction of bonds wasted in cycles. [h] ν_{eg} is the concentration of EANCs calculated from eq 23, ref 5 for the effective conversions X_I. [i] T_{eg} is the trapping factor calculated from eq A.3, A.7, and A.8 for the effective conversions X_I.

Results and Discussion

Theoretical Correlations between Quantities. A theoretical model for the alternating reaction $RA_2 + RB_3$ of monomers a and b with kinetically controlled cyclization, based on the statistical theory of branching processes and on the spanning-tree approximation,[5] gives relations between such quantities as, e.g., conversion, dilution during network formation, fraction of bonds wasted in elastically inactive cycles(s) weight fraction of the sol (w_s) or gel (w_g), and the concentration of elastically active network chains (EANC) in the gel (ν_{eg}) (cf. eq 5, 20, and 23, ref 5). In the Appendix, the theory[5] has been extended for calculation of the trapping factor T_{eg} (eq A.1–A.7) used in the Langley–Graessley approach of interchain constraints.

The extent of cyclization at the given composition and dilution (r_H, v_d^0) and conversion is determined by the parameter Λ

$$\Lambda = \frac{1}{N_A}\left(\frac{3\sum_i r_i}{2\sum_i Q_i r_i L_i^2}\right)^{3/2} \quad (3)$$

which characterizes the chain flexibility and thus also the cyclization probability. In this relation, $r_i = (r_a, r_b)$ is the number of atoms in the main chain in the shortest sequence joining two functional groups in monomers a and b, $Q_i = (Q_a, Q_b)$ is the number of atoms in the main chain of monomers a and b in the statistical segment, $L_i = (L_a, L_b)$ is the length per one atom of the main chain, and N_A is the Avogadro number. For the system MDI (component a) with PPT LHT-240 (component b) the values chosen for the calculation of $Q_a = 10$, $Q_b = 4.8$, $r_a = 13$, $r_b = 24.4$, $L_a = L_b = 0.15$ nm reflected fairly well[13] the dependence of the critical mole ratio of functional groups in gelation on dilution. The effect of dilution is expressed by the volume fraction of the polymer (includes the gel and sol) at the end of network formation v^0.

$$v^0 = 1 - v_d^0 \quad (4)$$

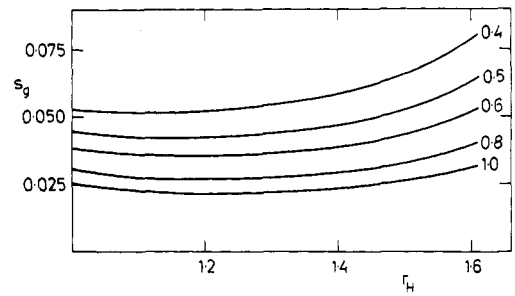

Figure 1. Calculated dependence of the fraction of bonds wasted in cycles in the gel, s_g, on r_H = [OH]/[NCO]. Numbers at curves denote the weight fraction of polymer $v^0 = 1 - v_d^0$.

It can be seen in Table I that the total fraction of bonds wasted in the cycles, s, varies about 1.5–2% at $v^0 = 1$ and about 4–5% at $v^0 = 0.4$, while the fraction of the same bonds in the gel, s_g, is somewhat higher (Figure 1). The weight fraction of the gel (w_g), the concentration of EANCs in the gel (ν_{eg}), and particularly the trapping factor (T_{eg}) decrease with increasing dilution. Within the framework of the model used, the dependence of ν_{eg} on w_g is universal and independent of r_H, dilution v^0, and conversion of isocyanate groups (Figure 2a). This universality has already been successfully used in correlating experiment and theory for polyurethane[12,17] and epoxide[23,24] networks as

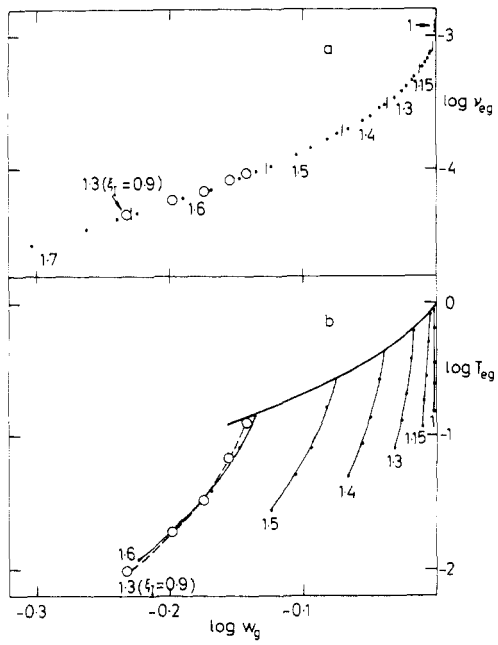

Figure 2. Calculated dependence of the concentration of EANCs ν_{eg} (mol cm^{-3}) and of the trapping factor, T_{eg}, on the weight fraction of the gel, w_g. (a) Dependence of ν_{eg} calculated by using eq 23, ref 5, for the variables r_H and $v^0 = 1 - v_d^0$; numbers at parts of the curve denote the intercept of constant values r_H ($\xi_I = 1$); O, values for $r_H = 1.3$ and $\xi_I = 0.9$. (b) Dependence of T_{eg} calculated by using eq A.3 for the variables r_H and $v^0 = 1 - v_d^0$; numbers at curves denote value r_H ($\xi_I = 1$); O, calculated T_{eg} values for $r_H = 1.3$ and $\xi_I = 0.9$.

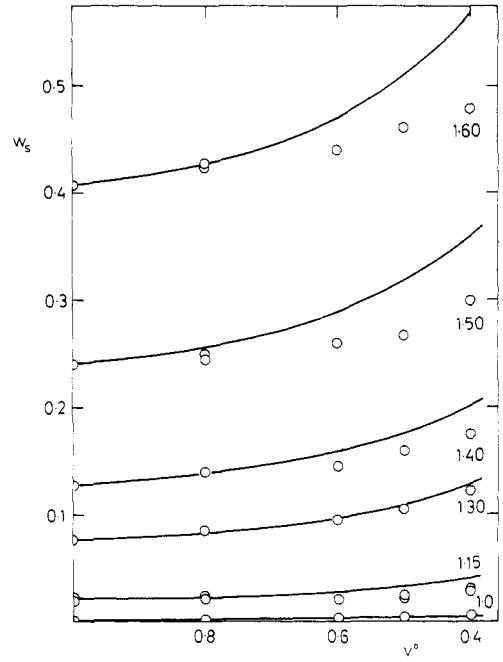

Figure 3. Dependence of the weight fraction of the sol, w_s, on the volume fraction of the polymer $v^0 = 1 - v_d^0$: (O) experiment; (—) theory eq 20, ref 5, for the constant effective conversion X_I found for networks with $v^0 = 1$; numbers denote r_H values.

it minimizes the effects of errors in the initial composition of the mixture or in the final conversion of minority groups. This universality, however, does not hold for the trapping factor T_{eg} (Figure 2b) because of its steep dependence on dilution (the explicit proportionality to $(v^0)^2$ (eq A.2) with a simultaneous decrease in the number of interacting segments). On the other hand, one can confirm a finding reported earlier that the dependence on w_g at constant v^0 is independent of conversion.[12] Figure 2 shows that the different dependences of T_{eg} and ν_{eg} on w_g can decide whether the contribution due to permanent interchain constraints to the equilibrium modulus plays an important role.

Weight Fraction of the Sol. The change in the weight fraction of the sol with dilution for various values of the mole ratio of OH and NCO groups r_H is given in Figure 3 and Table I. According to the theory,[5] w_s is determined by the cyclization parameter Λ (eq 3) and by the dilution given by v^0 and also by the fact that the real functionality of PPT, f_n, is lower than 3 (LHT-240 contains ~10 mol % of the bifunctional component, cf. also ref 12), while the theory has been formulated for $f_n = 3$.

Hence, to compare theory with experiment one should bear in mind the fact that $f_n < 3$. In view of the comparatively small deviation of f_n (=2.89) from three, it was not necessary to extend rigorously the theory described in ref 5 by introducing four further differential equations for the states of units of the bifunctional components of the commercial PPT. The following procedure was used instead: The effect of the functionality distribution on w_g is known in a ring-free system.[12] We assume that the deviation of functionality from 3 will affect equally the sol fraction in the ring-free system and in a system containing rings. It should hold, therefore, that

$$\frac{w_s^{f,c}}{w_s^{3,c}} = \frac{w_s^{f,0}}{w_s^{3,0}} \qquad (5)$$

where the upper indices f and 3 denote the functionality of PPT and c and 0 denote systems with and without cyclization. Hence, $w_s^{f,0}/w_s^{3,0}$ (obtained by using the procedure in ref 12) is the rescaling factor between the theoretical value, $w_s^{3,c}$, and the experimental one, $w_s^{f,c}$. By employing an iterative procedure, we search, at a given Λ, for the conversion of the minority groups that satisfies eq 5. The conversion values of isocyanate groups ξ_I calculated by using experimental values w_s (i.e., $w_s^{f,c}$) by means of eq 5 are summarized in Table I. It is obvious that these values are close to 100% and sometimes even exceed this value, but by less than 1%, which is most probably due primarily to experimental inaccuracies in the determination of w_s. It should be pointed out that in order to calculate other quantities, such as ν_{eg} and T_{eg}, no correction for the functionality distribution is needed, but it is possible to use the so-called effective conversion of isocyanate groups X_I, which transforms the effect of $f_n < 3$ into a decrease in conversion. This means that the X_I are calculated from the experimental w_s values directly from eq 20 in ref 5 (Table I).

The analysis indicates a considerable sensitivity of w_s to the final conversion of isocyanate groups. None of the existing analytical methods would allow us to distinguish reliably the concentrations of these groups in the gel at the level 0.1–1%. With respect to the experimental conditions used, it may be expected that the conversion of NCO groups in the system would be high, approaching 100% (OH groups in excess, the presence of a catalyst, etc.[12,14]). Thus, within the limits of experimental error the theory seems to describe adequately the sol content w_s as a function of r_H and v^0.

It is evident, nevertheless, that the calculated ξ_I values increase systematically with increasing dilution. If we assume a constant final conversion ξ_I found for the bulk state (Table I) also for diluted samples, we obtain the theoretical dependences shown in Figure 3 from which it might be derived that at higher dilutions the theory overestimates cyclization or the effect of the latter on w_s. This cannot be ruled out in view of the fact that the

spanning-tree approximation and the independence of the conformational probability of two groups meeting each other in the presence of already existing cycles become more inaccurate with increasing cyclization and thus dilution. To treat these deviations quantitatively, one would have to determine the final conversion of NCO groups with an accuracy of at least ±0.1%. It may be stated, however, that even with the simplifying assumption mentioned above and regarding the independence of ξ_I on v^0 the difference between theory and experiment never exceeds 10% of w_s.

Equilibrium Photoelastic Behavior. The equilibrium modulus is determined by the concentration of EANCs, dilution, and sol content. The stress–strain measurements can be performed on samples containing the diluent and sol, or on samples from which either the sol or diluent or both have been removed, or on those which are additionally swollen with an external swelling agent (cf., e.g., ref 25). The state of the network in any such state can be described by two factors: (1) the isotropic dilation (contraction) of network chains in the dry gel (sol and diluent have been removed) and (2) swelling degree of the gel (its volume fraction v_2), where the swelling agent can be the sol, the diluent, or an external swelling agent.

The dilation factor can be expressed by the volume fraction of the gel at the end of network formation v_g^0 (provided the densities of sol and gel are the same)

$$v_g^0 = V_{gel}/(V_{gel} + V_{sol}^0 + V_{dil}^0) = w_g v^0 \quad (6)$$

where V_{gel}, V_{sol}^0, and V_{dil}^0 are the volumes of the gel, sol, and diluent at the end of network formation, respectively.

The equilibrium modulus related to the isotropic state prior to measurement, G, is given by

$$G = A\nu_e(\langle r_i^2\rangle/\langle r_0^2\rangle)RT = A\nu_{eg}v_2^{1/3}(v_g^0)^{2/3}(\langle r_{nf}^2\rangle/\langle r_0^2\rangle)RT \quad (7)$$

where ν_e and ν_{eg} are the concentrations of EANCs per unit volume in the isotropic and dry extracted sample, respectively; $\langle r_i^2\rangle$, $\langle r_{nf}^2\rangle$, and $\langle r_0^2\rangle$ are respectively the mean-square end-to-end distances of EANCs in the isotropic, at network formation, and in the reference state; A is the front factor[9] the value of which for the phantom network is $A_{ph} = (f_e - 2)/f_e = {}^1/_3$ (f_e is the functionality of the cross-link), and for the real network with fully suppressed fluctuations of the cross-links, $A_{af} = 1$; R is the gas constant; and $v_2 = V_{gel}/(V_{gel} + V_{sol} + V_{dil} + V_{swell})$ is the volume fraction of the gel in the isotropic state before stress–strain measurement (V_{sol}, V_{dil}, and V_{swell} are volumes of the sol, diluent, and swelling agent in that state, respectively). Equation 7 has been derived assuming the validity $\langle r_i^2\rangle/\langle r_0^2\rangle = (V_i/V_0)^{2/3}$ and $\langle r_{nf}^2\rangle/\langle r_0^2\rangle = (V_{nf}/V_0)^{2/3}$.

In the case of measurements carried out with networks after completed cross-linking ($v_2 = v_g^0$, modulus G_p), from eq 7 we may write for the reduced modulus G_r^1 the relation

$$G_r^1 = A\nu_{eg}(\langle r_{nf}^2\rangle/\langle r_0^2\rangle) = G_p/w_g v^0 RT_1 \quad (8)$$

where $T_1 = 298$ K is the measurement temperature. In the case of measurements performed with the same samples after the evaporation of xylene (the sample still contains the sol, $v_2 = w_g$ and $v_g^0 = w_g v^0$, modulus G_d) at $T_2 = 333$ K, by the use of eq 7 the reduced modulus G_r^2 can be written as

$$G_r^2 = A\nu_{eg}(\langle r_{nf}^2\rangle/\langle r_0^2\rangle) = G_d/w_g(v^0)^{2/3}RT_2 \quad (9)$$

From eq 8 and 9 we have for the reduced ratio of the experimental moduli $\Omega = G_pT_2/G_dT_1 = (v^0)^{1/3}$; it can be seen in Figure 4 in which the average Ω values (obtained for networks with various r_H values) are plotted as a function of v^0 that the experimental data confirm the correctness of eq 7 (the slope equals ${}^1/_3$). Hence, within the limits of experimental error, $G_r^1 = G_r^2$.

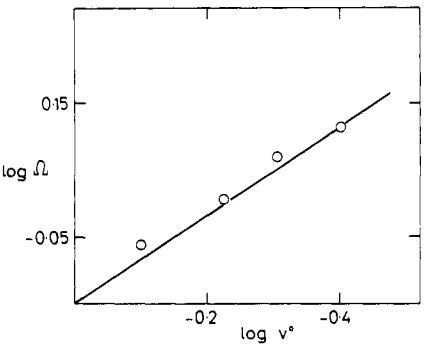

Figure 4. Dependence of the reduced ratio of the equilibrium moduli $\Omega = G_pT_2/G_dT_1$ on dilution $v^0 = 1 - v_d^0$: (O) experiment; (—) theory eq 7–9.

The values of the stress–optical coefficient of networks investigated after the preparation, C_p, are virtually independent of dilution and r_H (Table I). The same is true for the values of the stress–optical coefficient of networks investigated after drying, C_d. Generally, however, C_p is higher by 10–15% than C_d. Since the refractive index of xylene, $\bar{n}_x = 1.509$, is virtually the same as that of dry gels, the difference can be attributed to the different measurement temperatures of dry and swollen networks ($T_2/T_1 \sim 1.12$), so that the optical anisotropy of a statistical segment, $\Delta\alpha \sim CT$, is constant. The independence of $\Delta\alpha$ of v^0, r_H, and temperature is in agreement with the theoretical prediction for Gaussian networks and indicates the homogeneity and model character of the networks (each EANC due to the alternating mechanism of the reaction contains multiples of ${}^2/_3$(PPT + MDI)).

Concentration of Elastically Active Chains and the Theory of Rubber Elasticity. A comparison between the experimental reduced moduli G_r^1 and G_r^2 and the theoretical ν_{eg} values (calculated from eq 23, ref 15, for the effective conversions X_I determined from the sol values w_s, Table I) as a function of dilution for various constant r_H values is given in Figure 5. All experimental data lie in the range of front fractor values between $A = 1$ and $A = {}^1/_3$. While for $r_H = 1$ the reduced moduli are closer to the limiting value $A = 1$, for $r_H = 1.6$ they approach $A = {}^1/_3$. It may be deduced from Figure 5 that the decrease in the experimental moduli with dilution is larger than predicted by the theory for a constant value of the front factor. A steeper decrease in the modulus indicates the role played by the contribution of interchain interactions in the equilibrium modulus (cf. Figure 1); this problem is discussed in more detail below.

Assuming that the chemical contribution to the reduced modulus G_r is given by $\nu_{eg}/3$, the contributions of $\Delta = G_r - \nu_{eg}/3$ due to interchain constraints have been plotted in Figure 6 as a function of dilution, along with the theoretical prediction of ϵT_{eg} (T_{eg} was determined from eq A.3, A.6, and A.7 for the effective conversions X_I). The value of the constant $\epsilon = 5 \times 10^{-4}$ mol cm^{-3} determined earlier[12,14] was used in the calculation. While in the range of low r_H the theory predicts a faster decrease in Δ with v^0 than that determined experimentally, for higher r_H the fit between theory and experiment is better (however, for $r_H = 1.6$ the fit with theory would require $\epsilon \sim 2 \times 10^{-4}$ mol cm^{-3}). It may be said, however, that eq A.3 in the first approximation describes both the magnitude and the change of

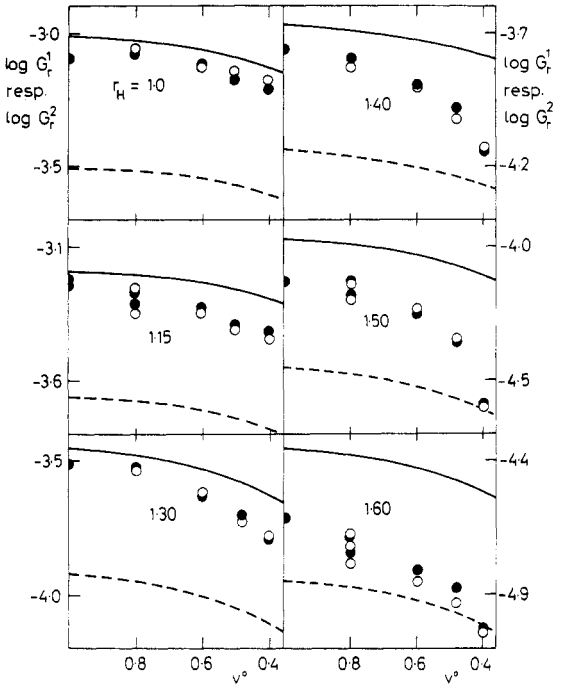

Figure 5. Dependence of the reduced moduli G_r (mol cm^{-3}) on dilution $v^0 = 1 - v_d^0$ for various r_H values. Experimental data: (○) G_r^1 (eq 8); (●) G_r^2 (eq 9); (—) theory with $A = 1$; (- - -) theory with $A = {}^1/_3$.

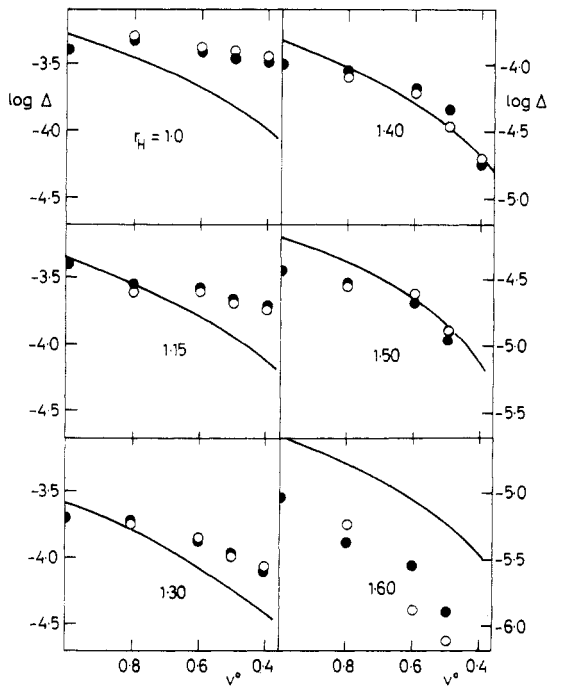

Figure 6. Dependence of the contribution from interchain constraints $\Delta = G_r - \nu_{eg}/3$ (mol cm^{-3}) on dilution $v^0 = 1 - v_d^0$ for various r_H values: (○, ●) experiment; (—) theoretical dependences of ϵT_{eg} with $\epsilon = 5 \times 10^{-4}$ mol cm^{-3}.

the topological contribution with dilution.

Generalized Dependence of the Concentration of EANCs on the Weight Fraction of the Gel, w_g. As has been discussed earlier, the generalized plot of log G_r as a function of log w_g reduces the inaccuracies in the determination of conversion ξ_I and r_H. In this case, however, the inaccuracy in ξ_I (X_I) is irrelevant because ν_{eg} and T_{eg} have been calculated directly from w_s. Also, in the generalized plot shown in Figure 7, the experimental moduli data lie between the limiting values of the front factor A = 1 and $A = {}^1/_3$ (similar to Figure 5); with increasing r_H the data are shifted to $A = {}^1/_3$. By comparing Figure 7 with the theoretically predicted dependence of ν_{eg} and T_{eg} on w_g shown in Figure 2, it may be concluded that the interchain interactions contribute to the modulus. Such a conclusion is also corroborated by the steep decrease in the experimental moduli with dilution for all r_H values.

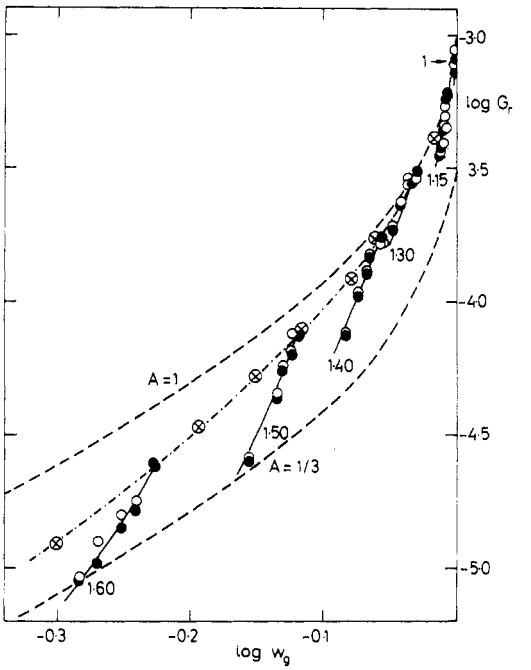

Figure 7. Generalized dependence of the reduced modulus G_r (mol cm^{-3}) on the weight fraction of the gel, w_g: (○, ●) experiment; (⊗) data obtained earlier[12] with undiluted networks, numbers at curves denote r_H values; (- - -) theory.

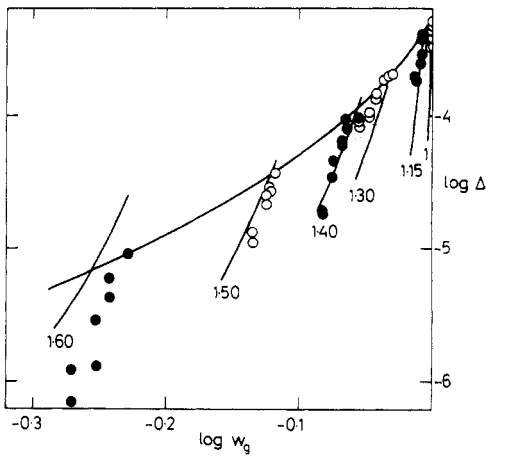

Figure 8. Generalized dependence of the contribution from interchain constraints Δ (mol cm^{-3}) on the weight fraction of the gel, w_g: (○, ●) experiment; (—) theoretical dependences of ϵT_{eg} with $\epsilon = 5 \times 10^{-4}$ mol cm^{-3}; numbers at curves denote r_H values.

The plot of the dependence of the experimental topological contribution $\Delta = G_r - \nu_{eg}/3$ on w_g together with the theoretical prediction ϵT_{eg} (where $\epsilon = 5 \times 10^{-4}$ mol cm^{-3} as before[12,14]) is given in Figure 8. It can be seen that in the range of low r_H the theory predicts a faster decrease than that found experimentally. On the other hand, for the highest $r_H = 1.6$ the fit between theory and experiment would require a lower value of the constant ϵ.

The assumption that the total effect of dilution on modulus is due to cyclization and not to reduction of permanent interchain constraints offers another alternative for interpretation of the results.[26] If it were so, the ex-

perimental lowering assuming $A = 1$ of the modulus by dilution would result in a drastic increase of the extent of cyclization over the value calculated by using the theory (Table I). Consequently, the sol fraction would be much larger than that calculated in Figure 3. Evidently, the experimental results (Table I, Figure 3) do not justify this approach. Moreover, if only cyclization was operative, the reduced modulus vs. gel fraction dependence should, according to the theory, converge to a single curve irrespective of dilution and stoichiometric imbalance. It should not be so if the weakening of interchain contraints comes into play (Figure 2). Figure 7 demonstrates the decomposition of the single curve into a family of curves caused by dilution, so that the latter approach seems to be correct.

The experimental elasticity data considered without regard to the sol fraction cannot rule out the applicability of other theories, e.g., Flory's theory[9] (with empirically adjusted change of the parameter κ on v^0 and r_H), because in networks from PPT LHT-240 the front factor A is always smaller than unity. It would also be of interest to correlate the results with the tube model (cf., e.g., ref 27). In conclusion, it may be said that the theory of trapped entanglements may be used to describe the experimental results, at least in the first approximation.

Appendix

Calculation of the Trapping Factor in the Theory of Trapped Entanglements for a Kinetically Controlled Stepwise Polyaddition of a Bi- and a Trifunctional Monomer Involving Cyclization. The trapping factor in the Langley–Graessley theory[10,11] of trapped entanglements was derived earlier for a ring-free system by using the theory of branching processes.[12] The trapping factor is proportional to the probability of pair contacts between segments situated in EANCs and those which are part of elastically active cross-links (eq A.21–A.27, ref 12).

According to eq A.21, ref 12, we have

$$T_e = N^{-1}[\sum_{i,j} C_{Hi(j)} + C_{I2(2)}]^2(v^0)^2 \qquad (A.1)$$

where $C_{Hi(j)}$ are numbers of interacting segments of poly(oxypropylene)triol or poly(oxypropylene)diol units issuing i bonds, of which j continue to infinity; $C_{I2(2)}$ is the number of segments of diisocyanate units issuing two bonds with infinite continuation; $v^0 = 1 - v_d^0$, v_d^0 is the volume fraction of the diluent during network formation. The squared expression in square brackets indicates that all pair interactions are considered. N is a normalizing factor such that $T_e = 1$ for a perfect network and $v^0 = 1$.

The numbers C_H and C_I in eq A.1 are proportional to the fractions of structural units, i.e., of units of triol (diol) and diisocyanate with different numbers of reacted groups. If, however, cyclization is involved, the structural units are represented by PPT and diisocyanate units that differ not only in their numbers of reacted groups (in the number of bonds issued) but also in whether these bonds are intermolecular or intramolecular. In ref 5, the fractions of these structural units are denoted with a_{ijk} (diisocyanate units) and b_{ijk} (PPT units); i, j, and k are the numbers of intermolecular bonds, intramolecular bonds (closing elastically inactive cycles), and unreacted functional groups, respectively. By analogy with eq A.1, we can write

$$T_e = [(n_a E_a + n_b E_b)^2(v^0)^2]/N \qquad (A.2)$$

$$T_{eg} = T_e/w_g \qquad (A.3)$$

where n_a and n_b are the mole fractions of units a (diisocyanate) and b (PPT) and E_a and E_b are the numbers of interacting segments of units a and b, respectively, related to unit a or b.

For a ring-free case, the definition of interacting segments is unambiguous (segments of EANCs and active cross-links), but with the case of existence of elastically inactive cycles their segments can either be excluded from or included in the interactions. In the former case (the segments of cycles not included), $T_{eg}^{(1)}$, we have

$$E_a = P_a a_{200}(1 - v_b)^2 \qquad (A.4)$$

$$E_b = P_b'(b_{201} + b_{210})(1 - v_a)^2 + b_{300}[3P_b'v_a(1 - v_a)^2 + P_b(1 - v_a)^3] \qquad (A.5)$$

and $N = n_a E_A$ (for $v_b = 0$) + $n_b E_b$ (for $v_a = 0$), where $P_a = 4$ (estimated); $P_b = M_b/M_{b0}$; $P_b' = (2/3)(M_b/M_{b0})$ (M_b is the molecular weight of PPT; M_{b0} is the molecular weight of a propylene oxide unit, 58) are the numbers of interacting segments provided by the respective units (the difference between P_b and P_b' is given by the fact that all three or only two branches of PPT are considered); v_a and v_b are the extinction probabilities;[5] and the coefficients a_{ijk} and b_{ijk} are the respective fractions of the units of components a and b issuing i intermolecular bonds and carrying j functionalities wasted in cycles and k unreacted functionalities.[5]

In the latter case (segments of cycles included), $T_{eg}^{(2)}$, we have

$$E_a = P_a a_{110}(1 - v_b) + P_a a_{200}(1 - v_b)^2 \qquad (A.6)$$

$$E_b = (P_b b_{120} + P_b' b_{111})(1 - v_a) + (P_b' b_{201} + P_b b_{210}) \times (1 - v_a)^2 + b_{300}[3P_b'v_a(1 - v_a)^2 + P_b(1 - v_a)^3] \qquad (A.7)$$

and $N = n_a E_a$ (for $v_b = 0$) + $n_b E_b$ (for $v_a = 0$). We found that the $T_{eg}^{(2)}$ values are higher by some 15–20% than those of $T_{eg}^{(1)}$. The experimental results were compared with the theoretical ones by using $T_{eg}^{(2)}$ values (Table I).

Registry No. (MDI)·(Niax LHT-240) (copolymer), 68541-67-3.

References and Notes

(1) Dušek, K. In *Developments in Polymerization*; Haward, R. N., Ed.; Applied Science: Barking, UK, 1982; Vol. 3.
(2) Dušek, K. *Rubber Chem. Technol.* **1982**, *55*, 1.
(3) Stepto, R. F. T. In *Developments in Polymerization*; Haward, R. N., Ed.; Applied Science: Barking, UK, 1982; Vol. 3.
(4) Temple, W. B. *Makromol. Chem.* **1972**, *160*, 277.
(5) Dušek, K.; Vojta, V. *Br. Polym. J.* **1977**, *9*, 164.
(6) Leung, Y.-K.; Eichinger, B. *J. Chem. Phys.* **1984**, *80*, 3877, 3885.
(7) Dušek, K.; Gordon, M.; Ross-Murphy, S. B. *Macromolecules* **1978**, *11*, 236.
(8) Stanford, J. L.; Stepto, R. F. T.; Still, R. H. In *Characterization of Highly Cross-Linked Polymers*; Dickie, R. A., Labana, S. S., Eds.; ACS Symposium Series 243; American Chemical Society: Washington, DC, 1984; p 1.
(9) Flory, P. J. *J. Chem. Phys.* **1977**, *66*, 5720.
(10) Langley, W. *Macromolecules* **1968**, *1*, 348.
(11) Pearson, D. S.; Graessley, W. W. *Macromolecules* **1980**, *13*, 1001.
(12) Ilavský, M.; Dušek, K. *Polymer* **1983**, *24*, 981.
(13) Matějka, L.; Dušek, K. *Polym. Bull. (Berlin)* **1980**, *3*, 485.
(14) Ilavský, M.; Dušek, K. *Polym. Bull. (Berlin)* **1982**, *8*, 359.
(15) Havránek, A.; Nedbal, J.; Berčík, Č.; Ilavský, M.; Dušek, K. *Polym. Bull. (Berlin)* **1980**, *3*, 497.
(16) Dušek, K.; Ilavský, M.; Matějka, L. *Polym. Bull. (Berlin)* **1984**, *12*, 33.
(17) Ilavský, M.; Bouchal, K.; Dušek, K. *Polym. Bull. (Berlin)* **1985**, *14*, 295.
(18) Dossin, L. M.; Graessley, W. W. *Macromolecules* **1979**, *12*, 123.
(19) Gottlieb, M.; Macosko, C. W.; Benjamin, G. S.; Meyers, K. O.; Merril, E. W. *Macromolecules* **1981**, *14*, 1039.

(20) Kirk, K. A.; Bidstrup, S. A.; Merrill, E. W.; Meyers, K. O. *Macromolecules* **1982**, *15*, 1123.
(21) Ilavský, M.; Prins, W. *Macromolecules* **1970**, *3*, 415.
(22) Ilavský, M.; Dušek, K. *Collect. Czech. Chem. Commun.* **1976**, *42*, 1152.
(23) Dušek, K.; Ilavský, M. *J. Polym. Sci., Polym. Phys. Ed.* **1983**, *21*, 1323.
(24) Ilavský, M.; Bogdanova, L. M.; Dušek, K. *J. Polym. Sci., Polym. Phys. Ed.* **1984**, *22*, 265.
(25) Ilavský, M.; Hasa, J.; Havlíček, I. *J. Polym. Sci., Polym. Phys. Ed.* **1972**, *10*, 1775.
(26) Stepto, R. F. T. *Polym. Prepr. (Am. Chem. Soc., Div. Polym. Chem.)* **1985**, *26*(2), 46.
(27) Heinrich, G.; Straube, E. *Acta Polym.* **1983**, *34*, 589.

Rheology of Model Polyurethanes at the Gel Point

Francois Chambon, Zoran S. Petrovic,† William J. MacKnight, and H. Henning Winter*

Polymer Science and Engineering Department and Chemical Engineering Department, University of Massachusetts, Amherst, Massachusetts 01003. *Received February 24, 1986*

ABSTRACT: The universality of the gel equation, a recently suggested rheological equation for polymers at the gel point, was tested on three well-defined cross-linking polyurethanes (PU). Stoichiometric amounts of triisocyanate cross-linker (DRF) were mixed with α,ω-dihydroxypoly(propylene oxides) (PPO) of nominal molecular weights 425, 1000, and 2000. As the cross-linking reaction progressed at 30 °C the evolution of the viscoelastic properties was measured. At the gel point, the storage modulus G' and the loss modulus G'' were found to be congruent and proportional to $\omega^{1/2}$, where ω is the frequency of the oscillatory shear experiment. The same behavior was previously observed with an end-linking poly(dimethylsiloxane), however, with tetrafunctional cross-linking points.[1,2] This suggests universal validity of the rheological equation for stoichiometrically balanced end-linking polymers.

Introduction

The gel point (GP) in network polymers is known to manifest itself by an infinite steady-shear viscosity and a zero equilibrium modulus.[3] In addition to that, Chambon and Winter[1,2] observed that a cross-linking poly(dimethylsiloxane) (PDMS) system at GP exhibits congruent moduli

$$G'(\omega) \sim \omega^{1/2} \sim G''(\omega) \tag{1}$$

and stress relaxation in a power law

$$G(t) \sim t^{-1/2} \tag{2}$$

These phenomena, including infinite steady-shear viscosity and zero equilibrium modulus, are described by the *gel equation*, which is a linear viscoelastic constitutive equation for the stress[2]

$$\tau(t) = S\int_{-\infty}^{t}(t-t')^{-1/2}\dot{\gamma}(t')\,dt' \tag{3}$$

where $\dot{\gamma}$ is the rate of deformation of the sample at GP. The only material parameter in the equation is the gel strength S.

The apparent simplicity and clarity of the gel equation suggests its universal validity for end-linking polymers with balanced stoichiometry. We therefore selected three polyurethanes (PU) and studied their rheology in the vicinity of GP. Similarly to the PDMS system which was used in the earlier experiments, these PU networks are also formed by an end-linking reaction of stoichiometrically balanced chemical species. However, the cross-linking process occurs by a different reaction and the cross-link functionality was chosen to be 3 instead of 4 for the PDMS. Nevertheless they are found to exhibit the same rheological behavior at GP as PDMS. This will be shown in the following.

Experimental Section

System. The constituents of the system are α,ω-dihydroxypoly(propylene oxide) (PPO) of nominal molecular weight 425, 1000, and 2000 and tris(4-isocyanatophenyl) thiophosphate (DRF), for which structural formulas are shown in Figure 1. The nominal molecular weight of the prepolymer was chosen far below the critical value for physical entanglements. Advantages of this system are that (i) the initial compounds are well characterized and can be readily obtained with a high degree of purity, (ii) the linear PPO component is available at different molecular weights with narrow polydispersity, (iii) the well-defined chemistry of the cross-linking process[4,5] makes it possible to form practically perfect networks, and (iv) the reaction kinetics at room temperature are slow.

Table I
α,ω-Dihydroxypoly(propylene oxide) (PPO) Characterization

sample	PPO425	PPO1000	PPO2000
$\bar{M}_n$ (VPO)	454	965	2018
$\bar{M}_w/\bar{M}_n$ (GPC)	1.013	1.007	1.006
functionality	1.93	1.88	1.94

Material Preparation and Characterization. Recent reports give details of sample preparation,[4] of curing kinetics, and of the properties of the final networks.[4-6]

PPO prepolymers (Aldrich Chemical Co.) were dried prior to use by azeotropic distillation with added benzene. The number-average molecular weights and the molecular weight distributions were measured[6] by VPO and GPC (Table I). The number of OH groups was determined by titration. In all three systems, the PPO prepolymers were found to be quasi-monodisperse ($M_w/M_n < 1.02$) and their functionality was very close to 2 (Table I).

The triisocyanate cross-linker was obtained from Mobay Chemical Co. in the form of a 20% solution in methyl chloride. After purification by recrystallization the NCO content was found to correspond to the expected theoritical value[6] of 27.1%.

The curing samples were prepared by mixing stoichiometric amounts of PPO and triisocyanate at 90 °C and under vacuum. After 5–10 minutes of mixing, the reacting samples were cooled to room temperature and transferred into the rheometer.

Rheological Experiments. Small strain oscillatory shear experiments were performed with a Rheometrics dynamic mechanical spectrometer using 25-mm-diameter parallel disks and a nitrogen atmosphere. All the samples were reacted isothermally at 30 °C. The evolution of the storage (G') and loss (G'') moduli

† Permanent address: Institut za Petrohemiju, Laboratorija za Polimere, Veljka Vlahoviča 2, Novi Sad, Yugoslavia.

0024-9297/86/2219-2146$01.50/0